

The Shapes of Bowed Interfaces in the Two-Dimensional Ising Model

Lee-Fen Ko¹ and Michael E. Fisher²

Received May 11, 1989

We show that properly normalized net energy fluctuations associated with interfaces in two-dimensional Ising models are described, asymptotically, by random walk partition functions. Two examples are investigated: one is a droplet on a wall, and the other is two nearby, ideally parallel interfaces; the mean shapes of the interfaces in both cases prove to be elliptic, bowed outward from the wall or from each other, the semiminor axis of the latter ellipse being $1/\sqrt{2}$ that of the former, in accord with random walk results.

KEY WORDS: Interfaces; 2D Ising model; random walks.

1. INTRODUCTION AND SUMMARY

In ref. 1, it is shown that random walk pictures and calculations can be used to study a great variety of interfacial problems in two-dimensional systems. It should be possible to reproduce those results by exact Ising model calculations. It is also desirable to identify which Ising variables correspond to the partial partition functions for random walks. The objective of the present work is to identify the appropriate Ising variable by exactly computing two specific problems concerning the shapes of equilibrium interfaces and, incidentally, to cross-check the random walk picture on a specific new problem.

For definiteness, we consider a 2D Ising strip of infinite length and height L , with spins $s_{i,j} = 1, -1$ at sites (i, j) . The horizontal and vertical reduced ferromagnetic couplings between nearest neighbor spins are K_h

¹ Department of Physics, Clarkson University, Potsdam, New York 13676.

² Institute for Physical Science and Technology, University of Maryland, College Park, Maryland 20742.

and K_v , respectively. In order to locate the interfaces, the expectation of some local variable or density is needed. We find that the *subtracted* energy density, or the energy fluctuation, is an effective object for the purpose³; in addition, we find that energy fluctuations coincide with random walk distributions in the asymptotic regime.

A (horizontal) energy density is the product of a pair of nearest neighbor spins,

$$\varepsilon_{n,m} \equiv s_{n,m-1} s_{n,m} \quad (1.1)$$

Hence it takes the value +1 for an ordered bond (with parallel spins) and -1 for a disordered or broken bond. A spin configuration can thus be specified by drawing lines connecting all the broken bonds. A typical configuration in a two-phase coexistence regime consists of many closed *bubbles* and one or more open, indefinitely long *interfaces*. The energy density expectation

$$\langle \varepsilon_{n,m} \rangle = \sum \varepsilon_{n,m} e^{-E/kT} / Z \quad (1.2)$$

where $Z = \sum e^{-E/kT}$ is the partition function subject to appropriate boundary conditions, measures the average presence of both the bubbles and the interfaces at site (n, m) . However, if we subtract from $\langle \varepsilon_{n,m} \rangle$ the pure-phase contribution, i.e., let $\langle \delta\varepsilon \rangle \equiv \langle \varepsilon \rangle - \langle \varepsilon \rangle_0$, where $\langle \cdot \rangle_0$ is expectation for the corresponding system without the interface, then the contribution from the bubbles is removed. This net energy fluctuation is then an effective tool for studying the location of the interfaces (see footnote 3). As an example, consider the case of a vertical interface extending from $(0, 0)$ to $(L, 0)$. It can be shown that asymptotically one has

$$\langle \delta\varepsilon_{n,m} \rangle \approx -2(2\pi b^2 L)^{1/2} \frac{e^{-m^2/2b^2n}}{(2\pi b^2 n)^{1/2}} \frac{e^{-m^2/2b^2(L-n)}}{[2\pi b^2(L-n)]^{1/2}} \quad (1.3)$$

where $b = (\sinh 2K_h / \sinh 2K_v \sinh \sigma)^{1/2}$, while the interfacial free energy is $\sigma = 2K_h + \ln \tanh K_v$. The behavior of the interface as $n \propto L \rightarrow \infty$ and $m \propto L^\delta$ for $\delta <, =, \text{ or } > 1/2$ which has been found from the local magnetization (refs. 4, 5, and 2, Section III. A) is completely captured in expression (1.3).

Aside from the first factor, the right-hand side of (1.3) is precisely the probability⁽⁶⁾ of one n -step walk and another independent $(L-n)$ -step

³ The suggestion that energy densities may be an appropriate tool for investigating interface profile locations has been made by Abraham (ref. 2, Section III. B). It has also been utilized recently by Abraham and Ko⁽³⁾ in an exact derivation of the modified Young equation for partial wetting in a two-dimensional Ising model.

random walk both going from the origin to the point m . This is not a coincidence, but a general rule. The interfacial behavior of exact Ising model results is strikingly similar to random walk behavior, as will be shown in this paper. The connection can be made precise by considering the energy fluctuation normalized by Z_0 , the pure-phase partition function, instead of by Z . Let $-\delta\varepsilon(n, m) \equiv (Z/Z_0)\langle\delta\varepsilon_{n,m}\rangle$; then (1.3) can be rewritten as

$$\delta\varepsilon(n, m) \approx 2Q_n^0(m) Q_{L-n}^0(m) \tag{1.4}$$

where $Q_n^0(m)$ is the asymptotic partial partition function of an n -step random walk⁽⁶⁾ from the origin to the point m , namely,

$$Q_n^0(m) = e^{-\sigma n} e^{-m^2/2b^2n} / (2\pi b^2 n)^{1/2} \tag{1.5}$$

Thus, the net energy fluctuation associated with interfaces should be normalized by the pure-phase partition function, in order to bring to forth the underlying random-walk character. Note that one might be tempted to associate the ratio of partition functions Z/Z_0 with a total partition function of random walks; but in fact, it is just another partial partition function of an L -step walk, in this case, which returns to the origin, i.e., $Z/Z_0 \approx Q_L^0(0)$.

We consider two problems concerning the shape of interfaces. The first is the shape of a droplet of width N lattice spacings on a wall, as sketched in Fig. 1.⁴ Let m and n be the distances along and from the wall as measured from one edge of the droplet. We find

$$\delta\varepsilon(n, m) \approx Q_m^W(n) Q_{N-m}^W(n) \tag{1.6}$$

⁴This problem has also been considered by Abraham and Issigoni,⁽⁷⁾ who studied the magnetization profile at the midpoint of the droplet and found that the mean interface position there was at a distance proportional to $N^{1/2}$ from the wall, in accord with our results: see below and ref. 1.

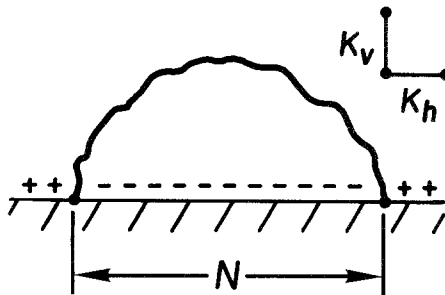


Fig. 1. A typical configuration of the interface for a droplet of overturned spins on a wall with its endpoints pinned by surface fields, as indicated.

where $Q_m^W(n)$ is the partition function of an m -step walk from an initial point at distance (measured in lattice spacings) of $n_0 = 1$ from an absorbing wall to a point at distance n , namely,

$$Q_m^W(n) = \frac{e^{-\sigma m}}{(\pi b^2/2)^{1/2}} \frac{ne^{-n^2/2b^2m}}{m^{3/2}} \quad (1.7)$$

See ref. 1. Note that for an anisotropic Ising model, σ and b depend on the anisotropy, and in this case they differ from those in (1.5) by an interchange of K_h and K_v . The formula (1.6) is precisely that predicted from random walk arguments;⁽¹⁾ hence the prediction of an *elliptic shape* for the most probable droplet configuration follows exactly for Ising models as well by the arguments of ref. 1 (Section 7.1).

The second problem we consider is two vertical interfaces^{(8),5} across the lattice with length of order L which are pinned N lattice sites apart, as shown in Fig. 2. However, if N is small, it is not correct to describe the situation as two vertical interfaces, for it becomes more favorable energetically for the interfaces to flip over into two horizontal ones, each fluctuating near one wall. Such behavior is not possible for more general types of interfaces, where, for example, there may be three different phases separated by the two vertical interfaces. Thus, we impose the restriction

⁵ It should also be noted that Abraham and Reed⁽⁵⁾ actually presented expressions for two interfaces at finite separation N in an Ising model in their study of a single interface; however, they analyzed in detail only the situation $N \rightarrow \infty$.

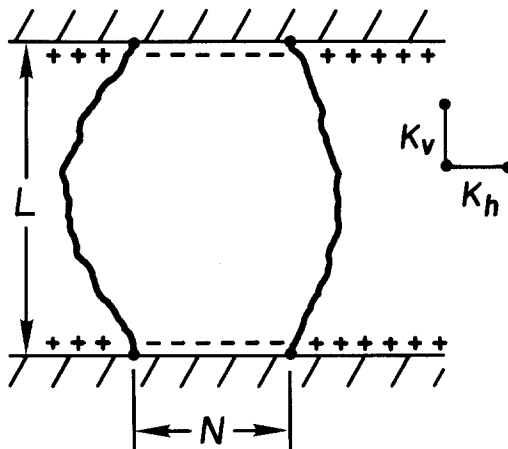


Fig. 2. A typical configuration for two nearby interfaces with pinned endpoints.

that such flipping is not allowed. This is done by considering $\tilde{Z} = Z - \lim_{L \rightarrow \infty} Z$, and a similar subtraction for $\delta\varepsilon$. Then we find that

$$\tilde{Z}/Z_0 \approx Q_L^0(0)^2 - Q_L^0(N)^2 \quad (1.8)$$

and

$$\begin{aligned} \delta\varepsilon(n, m) \approx & 2Q_L^0(0)[Q_n^0(m)Q_{L-n}^0(m) + Q_n^0(N-m)Q_{L-n}^0(N-m)] \\ & - 2Q_L^0(N)[Q_n^0(m)Q_{L-n}^0(N-m) + Q_n^0(N-m)Q_{L-n}^0(m)] \quad (1.9) \end{aligned}$$

The partition function ratio consists of the probability of independent random walkers, one of which walks from the origin to the origin, while the other walks from point N to point N in L steps, minus the probability that they cross each other to reach the other's destination. The loss of entropy amounts to a repulsion between the interfaces, and the distribution of $\delta\varepsilon$ in (1.9) reflects this fact by containing the negative terms, which concentrate more toward the center near the midpoint; hence the interfaces curve outward on the average. In the limit $N^2 \ll L \rightarrow \infty$, the most probable distribution is located at

$$2x^2 + (2b^2/L)y^2 = b^2L/2 \quad (1.10)$$

where $x = m - N/2$ and $y = n - L/2$. Thus, the mean shapes of interfaces in this case are also ellipses.⁶ Since the second fluctuating interface can bow away, it is not surprising that the ellipse here has a semiaxis reduced by a factor of $1/\sqrt{2}$ as compared with that for a droplet on a rigid wall. In fact, this factor can also be predicted precisely by the random walk methods of ref. 1, as we explain at the end of Section 5.

The rest of the paper is organized as follows: Section 2 introduces the transfer matrix method of Onsager⁽⁹⁾ and Kaufman⁽¹⁰⁾ for computing energy fluctuations; we show that they can be formulated in terms of Pfaffians of generating functions. Section 3 evaluates the generating functions. In Section 4, we investigate the asymptotic behavior of a typical generating function—the partition functions of random walks show up naturally. Section 5 finds the shapes of a droplet on a wall, and of two nearby interfaces.

⁶ It is worth remarking that the *spread* of a *single* interface going across a strip also has an elliptic character, as follows from Eq. (1.3) and from Abraham's analysis of the magnetization profile [see ref. 2, Section III. A, Eq. (3.6)] and indicated by the random walk analysis of ref. 1.

2. ENERGY FLUCTUATION IN TERMS OF GENERATING FUNCTIONS

Consider a square Ising lattice with spins $s_{i,j} = 1, -1$ at site (i, j) , $-M \leq i \leq M$, $0 \leq j \leq L$. Let the reduced couplings between nearest neighbor spins be K_v and K_h for the vertical and horizontal bonds, respectively, and the corresponding row-to-row transfer matrices be V_v and V_h . In terms of the Pauli matrices,⁽⁹⁾ we have

$$V_v = \exp\left(-K_v^* \sum_j \sigma_j^z\right), \quad V_h = \exp\left(K_h \sum_j \sigma_j^x \sigma_{j+1}^x\right) \quad (2.1)$$

where σ_j^α , $\alpha = x, y, z$, satisfies $[\sigma_k^\alpha, \sigma_j^\beta] = 0$ for $k \neq j$ and $\sigma_j^x \sigma_j^y = i\sigma_j^z$, etc.; and the dual couplings are given by $\cosh K_\alpha^* = \exp 2K_\alpha$. It is also useful to define the symmetrized transfer matrix V ,

$$V = V_h^{1/2} V_v V_h^{1/2} \quad (2.2)$$

Denote the state with all spins up (down) along a row as $|+\rangle$ ($|-\rangle \equiv \prod_j |\downarrow\rangle_j$); and the convention that $\sigma_j^x |\uparrow\rangle_j = \pm |\downarrow\rangle_j$ is used. The spin reversal operator $P_k^j = \prod_{i=k}^j (-\sigma_i^z)$ reverses the spins from the k th to the j th column. Then the partition function for a one-phase system Z_0 and for the systems of Figs. 1 and 2 (Z_1 for Fig. 1 and Z_2 for Fig. 2) can be expressed as

$$\begin{aligned} Z_0 &= \langle + | V^L | + \rangle, & Z_1 &= \langle + | P_0^{N-1} V^L | + \rangle, \\ Z_2 &= \langle + | P_0^{N-1} V^L P_0^{N-1} | + \rangle \end{aligned} \quad (2.3)$$

Similarly, expectations of energy density $\varepsilon_{n,m} = s_{n,m-1} s_{n,m}$ in the two systems are given by

$$\langle \varepsilon_{n,m} \rangle_1 = \langle + | P_0^{N-1} V^n \varepsilon_m^x V^{L-n} | + \rangle / Z_0 \quad (2.4)$$

$$\langle \varepsilon_{n,m} \rangle_2 = \langle + | P_0^{N-1} V^n \varepsilon_m^x V^{L-n} P_0^{N-1} | + \rangle / Z_0 \quad (2.5)$$

where $\varepsilon_j^x = \sigma_{j-1}^x \sigma_j^x$. Note that we normalize with the partition function Z_0 for the pure phase.

The transfer matrices can be put into a simple form in terms of anticommuting operators Γ_j , which satisfy $\Gamma_k \Gamma_j + \Gamma_j \Gamma_k = 2\delta_{kj}$ and are related to the Pauli matrices by⁽¹⁰⁾

$$\sigma_j^x = P_{-M}^{j-1} \Gamma_{2j}, \quad \sigma_j^y = P_{-M}^{j-1} \Gamma_{2j+1} \quad (2.6)$$

Then the relations

$$\varepsilon_j^x = \sigma_{j-1}^x \sigma_j^x = i\Gamma_{2j-1} \Gamma_{2j}, \quad \sigma_j^z = -i\Gamma_{2j} \Gamma_{2j+1} \quad (2.7)$$

lead to quadratic forms for the transfer matrices, namely,

$$V_v = \exp\left(iK_v^* \sum_j \Gamma_{2j} \Gamma_{2j+1}\right), \quad V_h = \exp\left(iK_h \sum_j \Gamma_{2j-1} \Gamma_{2j}\right) \quad (2.8)$$

Because we are interested only in “even” operators in the limit $M \rightarrow \infty$, the summations in (2.8) can be taken to be cyclic. To express the spin reversal operator in terms of the Γ ’s, the relations $\sigma_k^x \sigma_j^x |\pm\rangle = |\pm\rangle$ and $P_k^j = P_{-M}^{k-1} P_{-M}^j$ are used to obtain

$$\langle + | P_k^j = \langle + | \Gamma_{2k} \Gamma_{2j+2}, \quad P_k^j | + \rangle = \Gamma_{2j+2} \Gamma_{2k} | + \rangle \quad (2.9)$$

Then (2.3)–(2.5) can be expressed purely in terms of the Γ ’s.

An advantage of using the anticommuting operators is that we have available the thermodynamic Wick theorem^(11,12): Consider a set of operators O_p which are products of exponentials of bilinear expressions in the Γ ’s, namely,

$$O_p \equiv \prod_v^{\rho_p} \exp\left(\lambda_{pv} \sum_{m,n} A_{mn}^{pv} \Gamma_m \Gamma_n\right) \quad (2.10)$$

Then

$$\text{Tr}\left(\prod_{p=1}^{2s} \Gamma_{i_p} O_p\right) / \left(\prod_{p=1}^{2s} O_p\right) = \text{Pf}(\{X_{kl}\}) \quad (2.11)$$

where

$$X_{kl} = \text{Tr}\left[\left(\prod_{p < k} O_p\right) \Gamma_{i_k} \left(\prod_{k \leq p < l} O_p\right) \Gamma_{i_l} \left(\prod_{p > l} O_p\right) / \text{Tr}\left(\prod_p O_p\right)\right] \quad (2.12)$$

and the Pfaffian for the triangular array X_{kj} with $1 \leq k < j \leq 2s$ is defined by summing all possible contractions with a sign determined by the permutation P ,

$$\text{Pf}(\{X_{kj}\}) \equiv \sum_P (-1)^P \prod_{k=1}^s X_{P(2k-1) P(2k)} \quad (2.13)$$

In order to exploit the theorem, it is necessary to convert the matrix elements of (2.3)–(2.5) to traces. This can be done by gluing the top and bottom rows of the lattice and sending the horizontal couplings along that row to infinity. Since the spins in the row will be forced to line up in the limit, the two degenerate elements $\langle + | \cdot | + \rangle$ and $\langle - | \cdot | - \rangle$ are selected. Define

$$V_0 = \exp\left(K_0 \sum_j \sigma_j^x \sigma_{j+1}^x\right), \quad K_0 \rightarrow \infty \quad (2.14)$$

Then (2.3)–(2.5) are converted to the desired form of traces, according to

$$\begin{aligned} Z_0 &= \text{Tr}[V^L V_0], & Z_1 &= \text{Tr}[\Gamma_0 \Gamma_{2N} V^L V_0], \\ Z_2 &= \text{Tr}[\Gamma_0 \Gamma_{2N} V^L \Gamma_{2N} \Gamma_0 V_0] \end{aligned} \tag{2.15}$$

and

$$\langle \varepsilon_{n,m} \rangle_1 = i \text{Tr}[\Gamma_0 \Gamma_{2N} V^n \Gamma_{2m-1} \Gamma_{2m} V^{L-n} V_0] / Z_0 \tag{2.16}$$

$$\langle \varepsilon_{n,m} \rangle_2 = i \text{Tr}[\Gamma_0 \Gamma_{2N} V^n \Gamma_{2m-1} \Gamma_{2m} V^{L-n} \Gamma_{2N} \Gamma_0 V_0] / Z_0 \tag{2.17}$$

where $\lim_{K_0 \rightarrow \infty}$ is understood.

The role of the triangular array X_{kj} in (2.12) is played, in our problems, by the generating functions⁽¹³⁾ defined by

$$G(n, l)_{j,k} \equiv \lim_{K_0 \rightarrow \infty} \text{Tr}[V^n \Gamma_j V^{l-n} \Gamma_k V^{L-l} V_0] / \text{Tr}[V^L V_0] \tag{2.18}$$

The partition function for Fig. 1 follows just from the definition of the generating function, i.e., $Z_1/Z_0 = G(0, 0)_{0,2N}$, while the Wick theorem gives the subtracted energy density as

$$i\delta\varepsilon_1(n, m) = G(0, n)_{0,2m} G(0, n)_{2N,2m-1} - \{2m \leftrightarrow 2m-1\} \tag{2.19}$$

where $\delta\varepsilon_1(n, m) \equiv -\langle \varepsilon_{n,m} \rangle_1 + (Z_1/Z_0)\langle \varepsilon_{n,m} \rangle_0$; thus, the contributions from bubbles are removed, and the sign is changed so that the result is positive.

The two-interface partition function as given in (2.15) consists of three pieces in terms of the generating functions; two of them correspond to independent interfaces. If the interfaces are far apart, i.e., if $N \rightarrow \infty$, they behave like two independent vertical interfaces; in the opposite limit, the situation will be dominated by two horizontal interfaces of length of order N , each attaching to a wall. We disallow the latter situation by considering the subtracted partition $\tilde{Z}_2 = Z_2 - \lim_{L \rightarrow \infty} Z_2$. This restriction can be justified if we imagine that there are more than two phases being separated by the two interfaces as in a wetting situation^(1,14) or in systems undergoing a $p \times 1$ ($p \geq 3$) commensurate-incommensurate transition.⁽⁸⁾ Then this restricted partition function is given by

$$\tilde{Z}_2/Z_0 = G(0, L)_{0,0} G(0, L)_{2N,2N} - G(0, L)_{0,2N} G(0, L)_{2N,0} \tag{2.20}$$

A direct application of the theorem to the energy density given by (2.17) yields many terms. Here we apply the same restriction as in \tilde{Z}_2 and sub-

tract the pure phase part. If we denote the result by $\delta\varepsilon_2(n, m)$, we find, in terms of the generating functions,

$$\begin{aligned}
 i\delta\varepsilon_2(n, m) = & G(0, L)_{0,0} [G(0, n)_{2N,2m-1} G(n, L)_{2m, 2N} - \{2m \leftrightarrow 2m - 1\}] \\
 & + G(0, L)_{2N,2N} [G(0, n)_{0,2m-1} G(n, L)_{2m,0} - \{2m \leftrightarrow 2m - 1\}] \\
 & + G(0, L)_{2N,0} [G(0, n)_{0,2m} G(n, L)_{2m-1,2N} - \{2m \leftrightarrow 2m - 1\}] \\
 & + G(0, L)_{0,2N} [G(0, n)_{2N,2m} G(n, L)_{2m-1,0} - \{2m \leftrightarrow 2m - 1\}]
 \end{aligned}
 \tag{2.21}$$

The first (second) term is a one-interface term in the sense that the interface on the left (right) is disconnected from the energy operator; the last two terms describe the crossings. The generating functions are computed next.

3. EVALUATION OF THE GENERATING FUNCTIONS

First consider the special case $G(0, 0)_{j,k}$ in (2.18). By exploiting the anticommutation relation for the Γ 's and the cyclic property of a trace, one can establish^(12,13)

$$G(0, 0)_{j,k} = 2\delta_{j,k} - \text{Tr}[\Gamma_j V^L V_0 \Gamma_k] / \text{Tr}[V^L V_0]
 \tag{3.1}$$

If we commute Γ_j through $V^L V_0$ to the right in the second term, we get an equation for $G(0, 0)$. [Note that $G(n, l)_{j,k}$ can be considered as a matrix in (j, k) .] If

$$V_\alpha^{-1} \Gamma_j V_\alpha = \sum_k (R_\alpha)_{jk} \Gamma_k \quad \text{for } \alpha = h, v, 0
 \tag{3.2}$$

then

$$G(0, 0) = 2I - R^L R_0 G(0, 0) = 2(I + R^L R_0)^{-1}
 \tag{3.3}$$

where $R = R_h^{1/2} R_v R_h^{1/2}$. The matrices R_α can be computed from (2.8) using $\Gamma_k \Gamma_j + \Gamma_j \Gamma_k = 2\delta_{kj}$; the results are 2×2 block cyclic matrices. Let the (i, j) th block be denoted r_{i-j} . Then for the transfer matrices V_0, V_h we have $r_j = 0$ for $j \neq 0$, and

$$r_0 = \begin{pmatrix} \cosh 2K_\alpha & i \sinh 2K_\alpha \\ -i \sinh 2K_\alpha & \cosh 2K_\alpha \end{pmatrix}, \quad \alpha = 0, h
 \tag{3.4}$$

For the other transfer matrix V_v , one gets $r_j = 0$ for $j \neq 0, \pm 1$, and

$$r_0 = \begin{pmatrix} \cosh 2K_v^* & 0 \\ 0 & \cosh 2K_v^* \end{pmatrix}, \quad -r_1^t = r_{-1} = \begin{pmatrix} 0 & 0 \\ i \sinh 2K_v^* & 0 \end{pmatrix} \quad (3.5)$$

Block cyclic matrices can be diagonalized by Fourier transformation the same way as a scalar cyclic matrix. Thus, if $X = (x_{i-j})$ is a block cyclic matrix with x_{i-j} the (i, j) th block, one has

$$X(\omega) = \sum_{k=-M}^M x_k e^{-ik\omega} \quad (3.6)$$

where, in the limit $M \rightarrow \infty$, one obtains

$$x_k = \frac{1}{2\pi} \int_{-\pi}^{\pi} d\omega X(\omega) e^{ik\omega} \quad (3.7)$$

From (3.4)–(3.6) the Fourier transformations of the R_α matrices are found to be

$$R_\alpha(\omega) = \begin{pmatrix} \cosh 2K_\alpha & i \sinh 2K_\alpha \\ -i \sinh 2K_\alpha & \cosh 2K_\alpha \end{pmatrix}, \quad \alpha = h, 0 \quad (3.8)$$

and

$$R_v(\omega) = \begin{pmatrix} \cosh 2K_v^* & -i \sinh 2K_v^* e^{-i\omega} \\ i \sinh 2K_v^* e^{i\omega} & \cosh 2K_v^* \end{pmatrix} \quad (3.9)$$

Likewise, the matrix corresponding to the symmetric transfer matrix $V = V_h^{1/2} V_v V_h^{1/2}$ is given by

$$R(\omega) = R_h(\omega)^{1/2} R_v(\omega) R_h(\omega)^{1/2} = u(\omega) D(\omega) u(\omega)^{-1} \quad (3.10)$$

with

$$D(\omega) = \begin{pmatrix} e^{\gamma(\omega)} & 0 \\ 0 & e^{-\gamma(\omega)} \end{pmatrix}, \quad u(\omega) = \frac{1}{\sqrt{2}} \begin{pmatrix} e^{i\delta^*(\omega)/2} & -ie^{i\delta^*(\omega)/2} \\ -ie^{-i\delta^*(\omega)/2} & e^{-i\delta^*(\omega)/2} \end{pmatrix} \quad (3.11)$$

Here the functions $\gamma(\omega)$ and $\delta^*(\omega)$ are Onsager's well-known functions,⁽⁹⁾ which have the following factorized form:

$$\sinh \gamma(\omega) = \frac{\sinh 2K_h}{2 \sinh 2K_v} [(\alpha_1^{-1} - e^{i\omega})(1 - \alpha_1 e^{-i\omega}) \times (\alpha_2^{-1} - e^{i\omega})(1 - \alpha_2 e^{-i\omega})]^{1/2} \quad (3.12)$$

$$e^{i\delta^*(\omega)} = \left[\frac{(1 - \alpha_1 e^{i\omega})(1 - \alpha_2 e^{-i\omega})}{(1 - \alpha_2 e^{i\omega})(1 - \alpha_1 e^{-i\omega})} \right]^{1/2} \quad (3.13)$$

where $\alpha_1^{-1} = \exp 2(K_v + K_h^*)$, $\alpha_2^{-1} = \exp 2(K_v - K_h^*)$; and the branch of the square root is taken to be positive at $\omega = 0$.

On substituting (3.8), (3.10), and (3.11) in (3.3), the Fourier transform of $G(0, 0)$ can be readily computed. The general case $G(n, l)$, $0 \leq n \leq l \leq L$, can be obtained similarly by relating it to $G(0, 0)$ using (3.2); hence we obtain

$$G(n, l) = R^{-n}G(0, 0)R^l = 2(R^{n-l} + R^{L-l}R_0R^n)^{-1} \tag{3.14}$$

where we have used the property $R^{-1} = {}^T R$, the transpose of R . These Fourier transforms can be evaluated directly, since only 2×2 matrices are entailed. Note the simplifying relation resulting from the limit $K_0 \rightarrow \infty$, namely,

$$R_0(\omega)/A \rightarrow \begin{pmatrix} 1 \\ -i \end{pmatrix} \begin{pmatrix} 1 & i \end{pmatrix} \quad \text{as } A = e^{2K_0}/2 \rightarrow \infty \tag{3.15}$$

Thus, the final solution is given by

$$G(n, l)(\omega) = 2u(\omega) \begin{pmatrix} e^{-n_2\gamma(\omega)}\Phi^2(\omega) & -e^{-n_{11}\gamma(\omega)}\Phi(\omega) \\ -e^{-n_{12}\gamma(\omega)}\Phi(\omega) & e^{-n_0\gamma(\omega)} \end{pmatrix} \times u(\omega)^{-1} [1 + O(e^{-2L})] \tag{3.16}$$

where $\Phi(\omega) \equiv \tan[\delta^*(\omega)/2]$. Note that $n_0 = l - n$, $n_{11} = l + n$, $n_{12} = 2L - l - n$, and $n_2 = 2L - l + n$ represent the direct, one-image, and two-image separations. Finally, the Fourier transforms may be inverted to give

$$G(n, l)_{[j,k]} = \frac{1}{2\pi} \int_{-\pi}^{\pi} d\omega G(n, l)(\omega) e^{i(j-k)\omega} \tag{3.17}$$

where $G(n, l)_{[j,k]}$ denotes the 2×2 submatrix of $G(n, l)$ consisting of the $(2j - 1, 2j)$ th rows and the $(2k - 1, 2k)$ th columns. This expression and (3.16) constitute our general results for the generating functions.

4. ASYMPTOTICS OF THE GENERATING FUNCTIONS

If only the most dominant terms for the generating functions in (3.16) are retained, the $G(n, l)_{[j,k]}$ are functions only of $y = l - n \geq 0$ and $x = j - k$. Denote these 2×2 matrices as $F(x, y)$; we then have

$$F(x, y) = \frac{1}{2\pi} \int_{-\pi}^{\pi} d\omega e^{-y\gamma(\omega) + ix\omega} a_n(\omega)^\dagger a_l(\omega) \tag{4.1}$$

where the row vector is

$$a_k(\omega) = \begin{cases} (i-1) \sec \frac{1}{2} \delta^*(\omega), & k = 0, L \\ (ie^{-i\delta^*(\omega)/2} \quad e^{i\delta^*(\omega)/2}), & \text{otherwise} \end{cases} \quad (4.2)$$

while $a_k(\omega)^\dagger$ denotes the adjoint of $a_k(\omega)$. The singularities of the integrand in (4.1) are formed by a pair of branch cuts from $\gamma(\omega)$ and $\delta^*(\omega)$, as sketched in Fig. 3.

If $y \rightarrow \infty$, the integral in (4.1) is dominated by the saddle point at $\omega = 0$. This follows from the equation⁽⁹⁾

$$\cosh \gamma(\omega) = \cosh 2K_h \cosh 2K_v^* - \sinh 2K_h \sinh 2K_v^* \cos \omega \quad (4.3)$$

Therefore $\gamma(0)$ and $\gamma''(0)$ attain special significance; accordingly, we define

$$\begin{aligned} \sigma_v &\equiv \gamma(0) = 2(K_h - K_v^*) \\ b_v &\equiv \gamma''(0)^{1/2} = (\cosh 2K_v - \cosh 2K_h^*)^{-1/2} \end{aligned} \quad (4.4)$$

where the dual couplings satisfy $\sinh 2K \sinh 2K^* = 1$ and $\tanh 2K \cosh 2K^* = 1$. Since $\delta^*(0) = 0$, the asymptotics of the generating functions is found to be simply

$$F(x, y) \approx Q_y^0(x) \begin{pmatrix} 1 & -i \\ i & 1 \end{pmatrix} \quad (4.5)$$

where

$$Q_y^0(x) = e^{-\sigma_v y} e^{-x^2/2b_v^2 y} / (2\pi b_v^2 y)^{1/2} \quad (4.6)$$

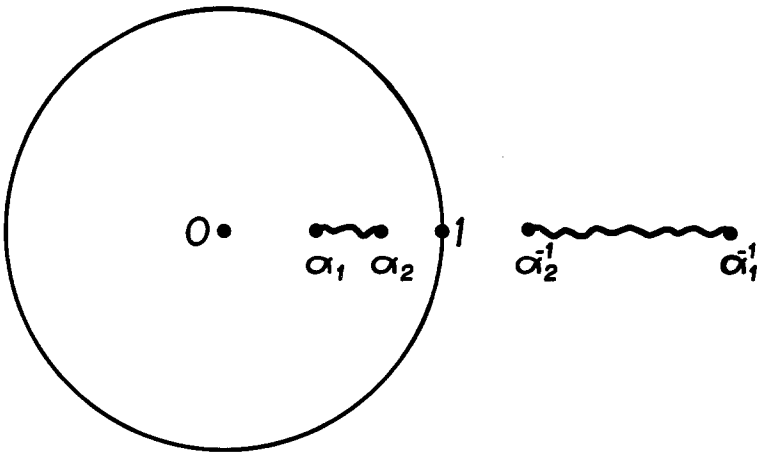


Fig. 3. The branch cuts for Onsager functions $\gamma(\omega)$ and $\delta^*(\omega)$ in the complex $\exp i\omega$ plane for $T < T_c$: See Eqs. (3.12) and (3.13).

Thus, each asymptotic generating function corresponds just to a random walk partition function, where σ_v and b_v are the single-step free energy and the mean step length, respectively.

On the other hand, if $x \rightarrow \infty$ (x can always be chosen positive) is desired, the contour of integration should be deformed around the branch cut, and the dominant part comes from near the branch point at $\exp i\omega = \alpha_2$. Define

$$\begin{aligned} \sigma_h &\equiv -\ln \alpha_2, & b_h &\equiv \lim_{v \rightarrow 0} \frac{(-2v)^{1/2}}{\gamma(\omega)}, \\ c &\equiv \lim_{v \rightarrow 0} \frac{e^{i\delta^*(\omega)}}{(-2v)^{1/2}} = \frac{b_h}{2} \sinh 2K_h \end{aligned} \tag{4.7}$$

where $v = -i\omega - \sigma_h$. As the notation suggests, σ_h and b_h are the same as σ_v and b_v , except that K_h and K_v are interchanged. In this case, the asymptotics of each element (k, j) of $F(x, y)$ typically has the form

$$\begin{aligned} F(x, y)_{k,j} &\sim \frac{1}{2\pi} \int_{-\pi}^{\pi} e^{-y\gamma(\omega) + ix\omega} e^{i\beta\delta^*(\omega)} \quad \text{for } \beta = 0, 1, -1 \\ &\approx -f(x, y) e^{-\sigma_h x} e^{-y^2/2b_h^2 x} / (2\pi)^{1/2} \end{aligned} \tag{4.8}$$

where one has

$$f(x, y) = \begin{cases} y/b_h x^{3/2}, & \beta = 0 \\ c(y^2/b_h^2 - x)/x^{5/2}, & \beta = 1 \\ 1/cx^{1/2}, & \beta = -1 \end{cases} \tag{4.9}$$

Note that the case $\beta = 0$ gives the partition function of a random walk near an absorbing wall, $Q_x^W(y)$; see (1.7) and ref. 1.

5. SHAPES OF INTERFACES

The ratio of partition functions and the energy fluctuation for a droplet on a wall are found from (2.19), (4.1), (4.2), and (4.7)–(4.9) to be

$$\frac{Z_1}{Z_0} \approx 2b_h c Q_N^W(1), \quad \delta\varepsilon_1(n, m) \approx Q_m^W(n) Q_{N-m}^W(n) \tag{5.1}$$

Thus, $\delta\varepsilon_1$ is precisely described by two independent walks as predicted in ref. 1; hence the elliptic shape of the most probable droplet configuration follows exactly as shown there.

For the case of two interfaces, we use (2.20), (2.21), (4.1), and (4.5). The ratio of partition functions is simply

$$\tilde{Z}_2/Z_0 \approx Q_L^0(0)^2 - Q_L^0(N)^2 \quad (5.2)$$

Thus, the partition function is reduced from that for two independent walkers to reach their respective destination across the strip, by the amount for the walkers to cross and reach the other's destination independently. This reduction in partition function, or loss of entropy, amounts to a repulsive force between the interfaces, as expected.^(1,15) For the local probability distribution the result for the energy fluctuations is

$$\begin{aligned} \delta\varepsilon_2(n, m) \approx & 2Q_L^0(0)[Q_{L/2+y}^0(N/2+x) Q_{L/2-y}^0(N/2+x) + \{x \rightarrow -x\}] \\ & - 2Q_L^0(N)[Q_{L/2+y}^0(N/2+x) Q_{L/2-y}^0(N/2-x) + \{x \rightarrow -x\}] \end{aligned} \quad (5.3)$$

where $y = n - L/2$ and $x = m - N/2$ are distances measured from the center of the two interfaces. The two terms here correspond to the two terms in (5.2). The maxima of the first term are near $x = \pm N/2$. The negative probability represented by the second term is concentrated more closely on the center; hence the net distribution bulges outward, as is consistent with the repulsion picture.

Writing (5.3) out in detail yields

$$\begin{aligned} \delta\varepsilon_2(n, m) \approx & \frac{4e^{-2L\sigma}}{b_v^2(2\pi)^{3/2} [Lz(y)]^{1/2}} e^{-L(N^2 + 4x^2)/8z(y)} \\ & \times \left(\cosh \frac{NLx}{2z(y)} - e^{-N^2/2b_v^2L} \cosh \frac{Nyx}{z(y)} \right) \end{aligned} \quad (5.4)$$

where $z(y) \equiv b_v^2[(L/2)^2 - y^2]$. In the limit $N^2 \ll L$, we may expand the functions in the parenthesis for small arguments; the most probable distribution is again found to be an ellipse, namely,

$$2x^2 + (2b_v^2/L) y^2 = b_v^2 L/2 \quad (5.5)$$

Compared with the ellipse for a droplet on a wall, the semiaxis here is reduced by a factor of $1/\sqrt{2}$. This is consistent with the idea that the other interface is not rigid and so is also repelled.

The result (5.5) can also be anticipated by random walk methods. The effective potential of repulsion $W(l)$ between an interface/walk of diffusivity b^2 and a wall at distance l is $\frac{1}{2}k_B T b^2/l^2$, while between two interfaces/walks of diffusivities b_1^2 and b_2^2 , it is⁽¹⁾ $\frac{1}{2}k_B T(b_1^2 + b_2^2)/l^2$. Thus, the interface repulsion is strengthened. However, one must compare the distance of separa-

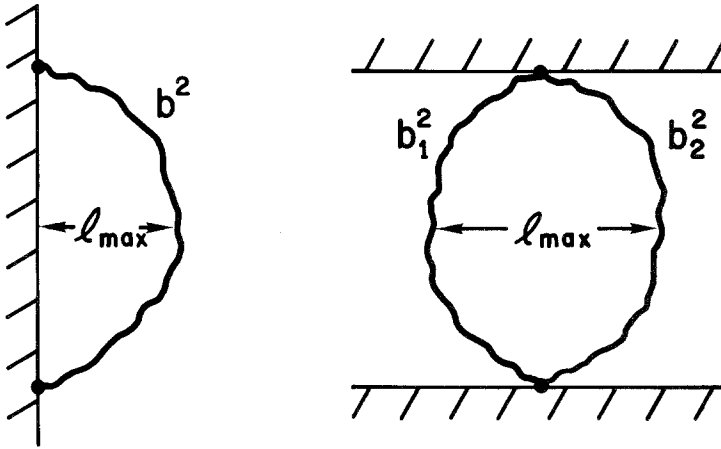


Fig. 4. In the random walk picture, the interface of Fig. 1 can be described by a walker of diffusivity b^2 where the maximum separation with the wall l_{\max} is the semiaxis of an ellipse. The interfaces of Fig. 2, for $N^2 \ll L$, are described by two walkers of diffusivities b_1^2 and b_2^2 ($b_1 = b_2$ here), where l_{\max} is the complete axis.

tion in each case, which, at maximum, represents the semiaxis in the wall case, but constitutes the complete axis for two interfaces: See Fig. 4. Thus, the equation of the ellipse in the wall case goes over to that for the two interfaces by a replacement of $x \rightarrow 2x$ and $b^2 \rightarrow 2b^2$ (with $b_1 = b_2$). This leads precisely to (5.5) and, hence, to the factor $1/\sqrt{2}$. The full distribution for two (possibly dissimilar) interfaces can also be found from ref. 1, in analogy to (1.6), if (1.7) is replaced by the distribution for two distinct vicious walkers [see Eq. (4.18) of ref. 1].

ACKNOWLEDGMENTS

M.E.F. is grateful to the National Science Foundation for support through the Condensed Matter Theory Program under grant DMR 87-96299. Dr. Douglas B. Abraham and Dr. Helen Au-Yang kindly commented on the manuscript. The encouragement and stimulation provided by Dr. D. B. Abraham in collaborative work on related problems and by Dr. Gabor Forgacs through several discussions have been deeply appreciated by L.F.K.

REFERENCES

1. M. E. Fisher, *J. Stat. Phys.* **34**:667 (1984).
2. D. B. Abraham, in *Phase Transitions and Critical Phenomena*, Vol. 10, C. Domb and J. L. Lebowitz, eds. (Academic Press, New York, 1986).

3. D. B. Abraham and L. F. Ko, *Phys. Rev. Lett.* **63**:275 (1989).
4. D. B. Abraham and P. Reed, *Phys. Rev. Lett.* **33**:377 (1974).
5. D. B. Abraham and P. Reed, *Commun. Math. Phys.* **49**:35 (1976).
6. W. Feller, *An Introduction to Probability Theory and its Applications*, Vol. 1 (Wiley, New York, 1950).
7. D. B. Abraham and M. E. Issigoni, *J. Phys. A* **13**:L89 (1980).
8. D. A. Huse, A. M. Szpilka, and M. E. Fisher, *Physica* **121A**:363 (1983); D. A. Huse and M. E. Fisher, *Phys. Rev. B* **29**:239 (1984).
9. L. Onsager, *Phys. Rev.* **65**:117 (1944).
10. B. Kaufman, *Phys. Rev.* **76**:1232 (1949).
11. M. Gaudin, *Nucl. Phys.* **15**:89 (1960); E. H. Lieb, *J. Comb. Theory* **5**:313 (1968); E. R. Smith, *J. Phys. C* **3**:1419 (1970).
12. J. H. H. Perk and H. W. Capel, *Physica* **89A**:265 (1977).
13. H. Au-Yang and L. F. Ko, unpublished; see also: L. F. Ko, Ph. D. thesis, State University of New York, Stony Brook (1986), unpublished; B. M. McCoy and J. H. H. Perk, in *Lecture Notes in Mathematics*, Vol. 925, D. Chudnovsky and G. Chudnovsky, eds. (Springer-Verlag, Berlin, 1982), p. 12.
14. M. R. Moldover and J. W. Cahn, *Science* **207**:1073 (1980).
15. D. S. Fisher, M. P. A. Fisher, and J. D. Weeks, *Phys. Rev. Lett.* **48**:369 (1982).